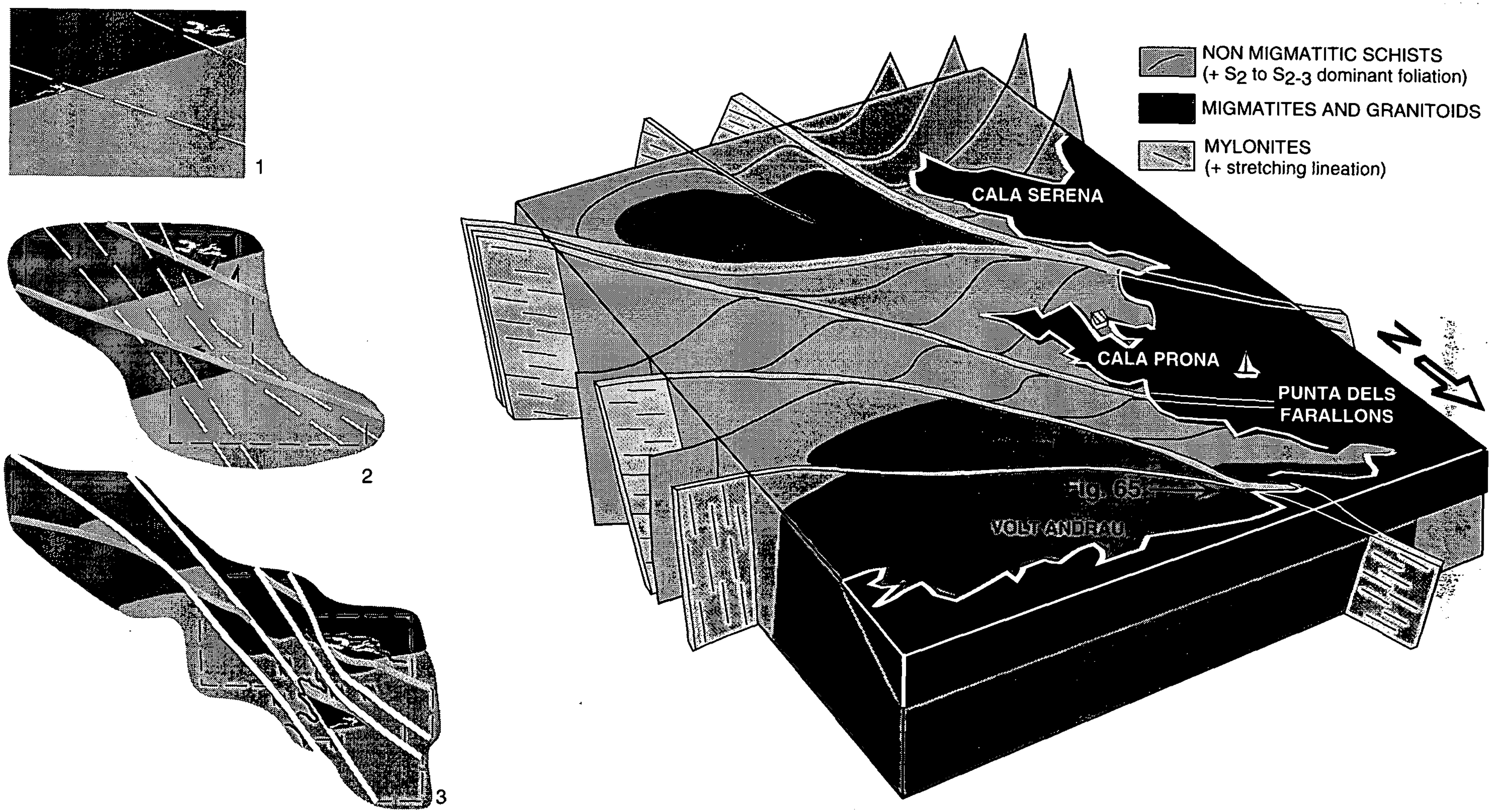

Fig. 64. Block-diagram of the Punta dels Farallons migmatite complex showing the main attitude of the late shear zones in this area. Left: kinematic interpretation for the present configuration of the migmatite complex. 1. Pre-mylonitic stage, 2. Displacements produced by sinistral and normal shearings. 3. Final result after dextral shearing. Pegmatite dykes are shown in white (After Carreras & Druguet 1994b).

5 RELATIONSHIPS BETWEEN DEFORMATION, METAMORPHISM AND MAGMATISM

5.1. METAMORPHISM AND DEFORMATION

The metamorphic conditions at which rocks were deformed have been used in previous sections as a tool to separate different deformational events. In this chapter, an outline is given on the relations between metamorphism and deformation events. The present space distribution of prograde and retrograde metamorphic zones (Fig. 11) must be the response to a complex evolutive pattern, with metamorphism being not only progressive in space but also in time. Main relationships between metamorphism and deformation are expressed in Fig. 66. In spite of some available quantitative data on temperature and pressure conditions of metamorphism, more systematic analysis is needed, and accurate reconstruction of the tectono-PTt evolution has not been accomplished yet.

Despite a possible incipient metamorphism predating the D_1 event, the regional prograde metamorphism approximately started during this deformation event. At these firsts steps, metamorphism probably did not exceed the greenschists facies conditions (or the lower amphibolite facies at the most). The possibility of staurolite growing during D_1 deformation is open, since, where observed, it is always replaced by andalusite or cordierite + sillimanite. The abundance of pre- to syn-D_1 quartz segregation veins is indicative of these first metamorphic stages, which would involve many dehydration reactions for water-saturated rocks of the sedimentary sequence.

The observed relationships between mineral growth and deformation indicates that the blastesis of most minerals postdates D_1 deformation. In this way, most porphyroblasts (cordierite, andalusite, garnet) grew when S_1 foliation was already well developed, at an stage between D_1 and D_2. The half-dome shaped macrostructure that formed in this intermediate stage might be associated to this episode. However, the lack of meso- and microstructures related to the macrostructure hinders to unravel the question.

For rocks located in the biotite and cordierite-andalusite zones, the maximum metamorphic conditions were reached during this intermediate episode between D_1 and D_2, and remained constant until the end of the D_2 event. For rocks located in the sillimanite and sillimanite-K-feldspar zones, peak metamorphic conditions occurred a bit later between D_2 and $D_{2\text{-}3}$ event, since sillimanite and K-feldspar grew synkinematically during D_2 and $D_{2\text{-}3}$ folding. Therefore, it can be assumed that higher grade zones formed later than lower grade ones, which achieved stable temperature conditions for longer periods. The prevalent succession of mineral associations in the entire area is a typical indicator for a metamorphism prograding from low to high temperature (high thermal gradient) at low pressure conditions. D_2-related structural zonation would take place simultaneously, together with migmatization and emplacement of calc-alkaline granitoids in domains of high D_2 strain and higher grade (upper amphibolite facies). Metamorphism, at least at this stage, seems to be intimately related in both space and time to the emplacement of such intrusive rocks.

Retrogression of metamorphism approximately started at the time of $D_{2\text{-}3}$ deformation. Pegmatites were emplaced just following peak metamorphism and, in relation with them, coarse muscovitization took place in the surrounding metasediments. The $D_{2\text{-}3}$ event was therefore contemporaneous with high temperature retrogression in the northern area. The vertical cylindrical folding structure initiated in the D_2 event, continued during this stage, producing a decompressional effect on the rocks located at the northern high strain zones, accompanied by a slow temperature drop. In some specific localities, the temperature drop might had worked faster than decompression during retrogression, so that some rocks would have passed through the kyanite stability field. This could be a possible explanation for the local presence of kyanite replacing prograde assemblages, specially along the pinched hinge of the southern synform in La Birba road area.

Retrogression was more significant during D_3, i.e. specially developed around late folds and shear zones, where low metamorphic grade conditions were newly reached. At this stage, the set of intrusive granitoids, included the pegmatite dyke swarm, would be completely crystallized, being able to deform at a low temperature solid state.

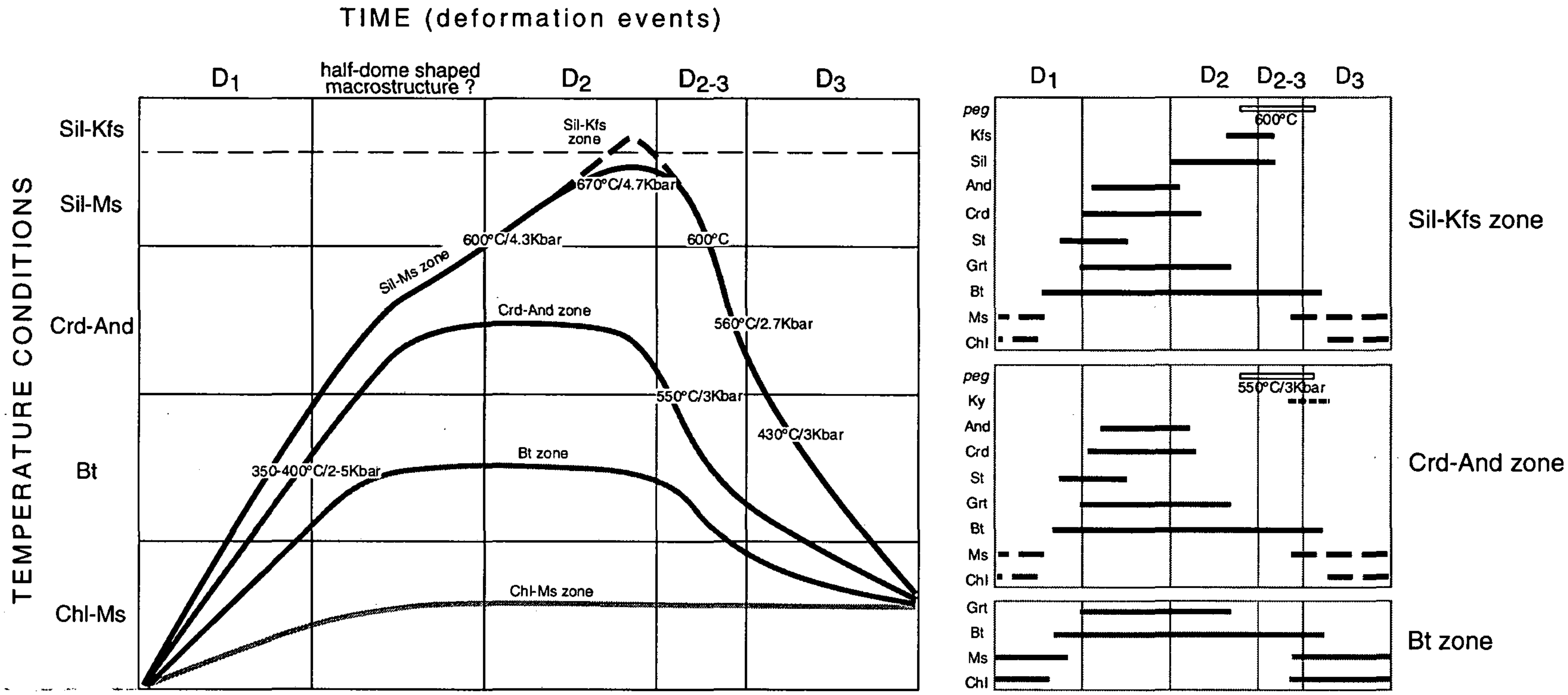

Fig. 66. Sketches showing relations between successive metamorphic zones and deformation events. The plot in the left side shows the metamorphic evolution of mapped metamorphic zones. In the right side, the relative time of blastesis of different minerals are plotted for three different metamorphic zones. *peg* = pegmatites.

5.2. MIGMATITE COMPLEXES AND DEFORMATION*

The Punta dels Farallons and Tudela areas correspond to domains of progressive D_2 to D_{2-3} high strain, as the Culip-Cap de Creus example. However, whereas in the Culip-Cap de Creus area deformation started at low D_2 strain and progressed while increasing strain to high D_{2-3} strain, in the areas surrounding the migmatite complexes the D_2 deformation event already produced high strain domains which consecutively progressed into D_{2-3} structures. The problem of labelling deformational stages is the same in both examples and thus it is difficult to separate D_2 from D_{2-3}. Although, in general, deformation affecting the metasediments within and surrounding these complexes is rather homogeneous, small variations in intensity leads to the recognition of sub-areas of high (possibly D_2) and very high (possibly D_{2-3}) strain, with the second type sub-areas located closer to the migmatite complexes.

The Punta dels Farallons example (Fig. 67) has been used in the following sections to deepen in the relationships between deformation, migmatization and magmatic processes. This area corresponds to a migmatite complex located in the northernmost outcrops within the larger high strain domain, and it is possibly close to its core. Moving northwards towards any of the migmatite outcrops, the S_2 foliation increases in penetrativity (decreases in spacing), and the foliation patterns show an apparently dextral geometry, in which the axial traces of the folds change from NE-SW to E-W trending in the highest strain zones (stereoplots from domains A, B & C), indicating a non-coaxial rotational component in the deformation. Within the zones of highest strain, a steeply plunging stretching lineation is associated with a steeply north-dipping fabric. The steeply plunging F_2 folds become tighter towards these zones, until they are totally transposed.

*Part of this section was submitted to J. Struct. Geol. (Druguet & Hutton).

5.2.1. MAGMATISM AND DEFORMATION

The calc-alkaline sequence

The basic-intermediate types contain an internal deformational fabric consisting of an alignment of hornblende, biotite and plagioclase. This is a magmatic or sub-magmatic-state fabric (i.e. formed during or in the latest stages of crystallization) in the center of the bodies, and it becomes increasingly a high temperature solid-state fabric (i.e. early post-crystallization deformation) as it intensifies towards the contacts with the enclosing schists, where it can be correlated with the pervasive fabric (Fig. 68 and Fig. 69a). This magmatic to solid state fabric (which trends between E-W and NW-SE and dips steeply north) is parallel to the different compositional heterogeneities (Fig. 69b) and to the margins of the lensoid bodies. In granitoids with fold-like shapes the fabric is axial planar to these folds. A predominantly steeply plunging stretching lineation is sometimes associated with the granitoid fabric, and whereso it is sub-parallel to the lineation in the enclosing metasediments. These relationships imply that emplacement of these bodies took place during the regional D_2 deformation.

The bodies and veins of granodiorite and granite all contain magmatic to solid-state deformation fabrics which may be correlated with the foliation in the enclosing metasediments.

A variety of features, providing constraints to the timing of emplacement and deformation, is displayed by these minor intrusions. The veins and sheets may be sub-parallel or slightly oblique to the external foliation (in these cases they are straight or boudinaged) or else highly oblique (in which case they are folded). In the folding case, the internal magmatic fabric is continuous with the external foliation, as in the basic-intermediate igneous bodies (Fig. 70a). In the slightly oblique veins and sheets the internal magmatic fabric is, in most cases, also slightly oblique to the vein walls (Fig. 70b). The bodies usually contain small xenoliths of the enclosing metasediments which carry D_2 deformation features (crenulation cleavage and folds). In addition, the xenoliths may be sometimes aligned parallel to, or elongated by, the internal magmatic fabrics. These relationships suggest that the igneous bodies were intruded while the D_2 deformation event was occurring and were subsequently deformed by it.

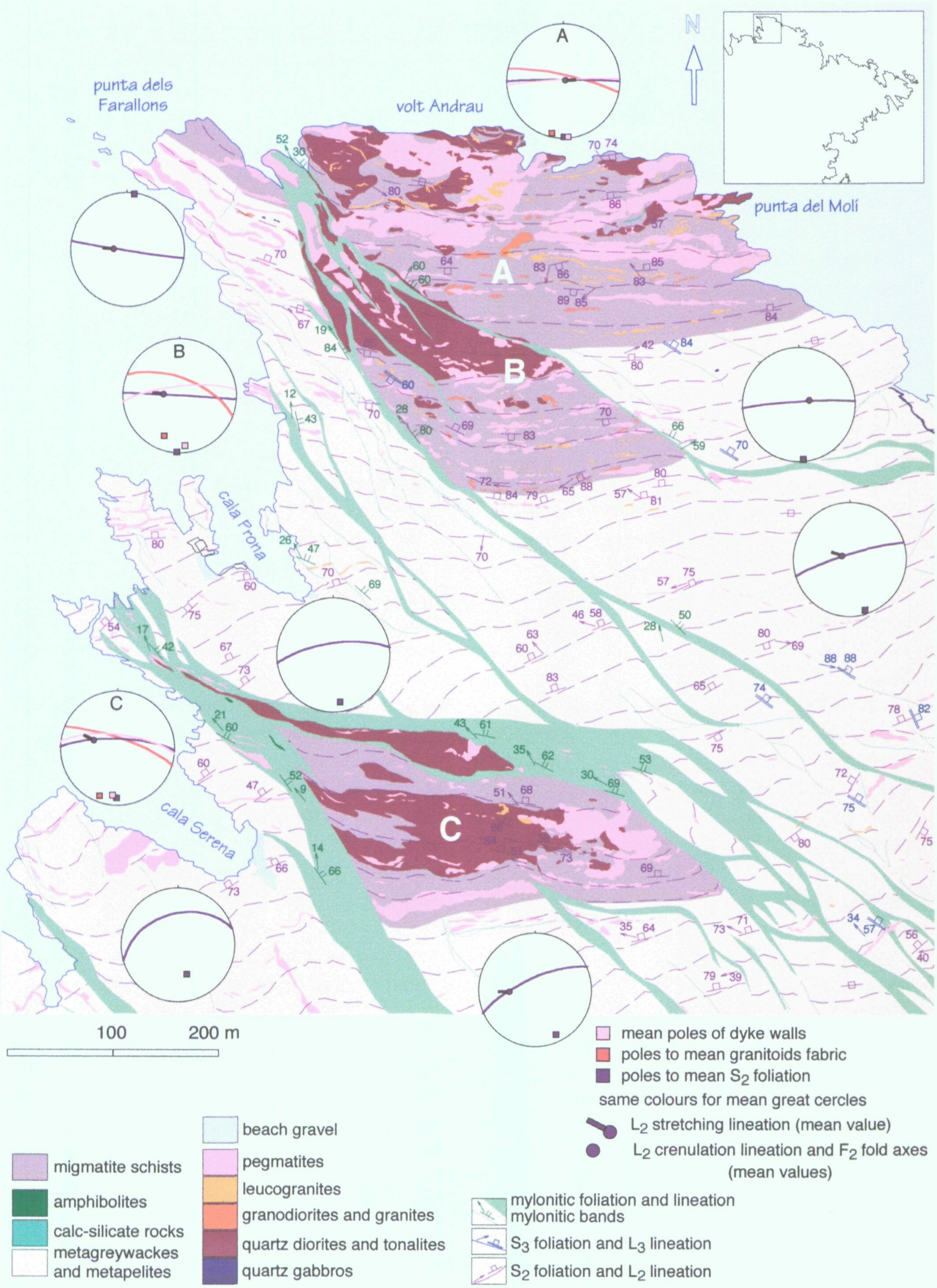

Fig. 67. Structural map of the Punta dels Farallons migmatite complex and surrounding domains. A, B and C: migmatite outcrops.

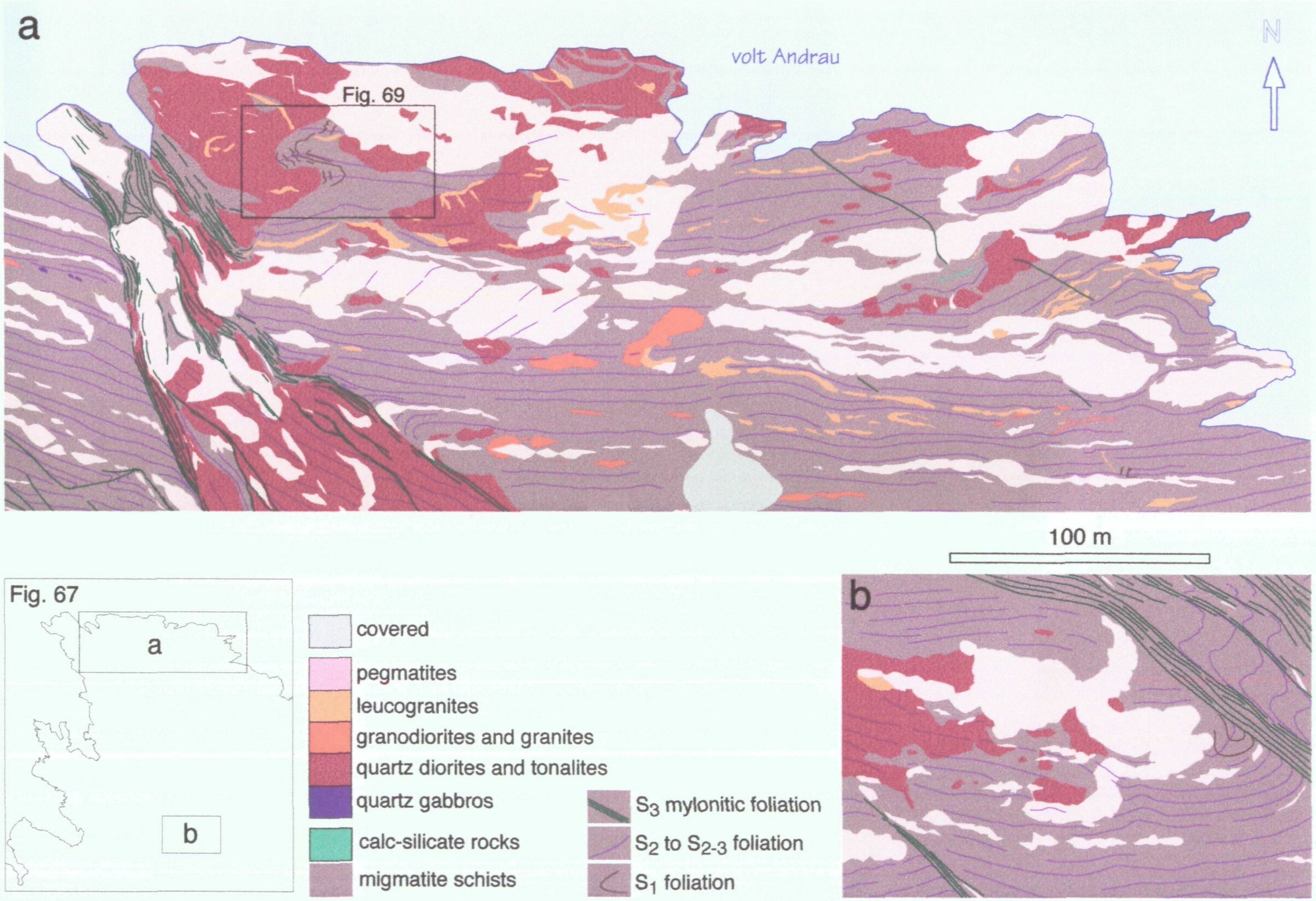

Fig. 68. Detail maps of granitoids and pegmatites from the Punta dels Farallons migmatite complex. (a): Volt Andrau outcrops, (b): east Cala Serena outcrops.

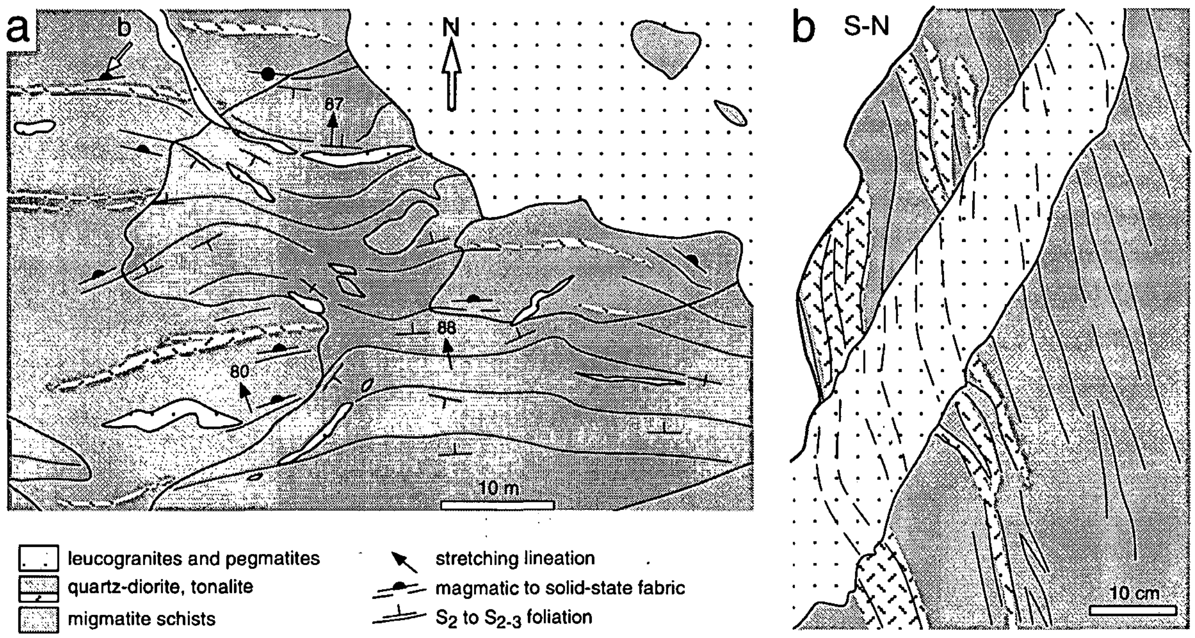

Fig. 69. Detail map (a) and field sketch (b) of one of the basic-intermediate bodies. Locations are shown in Fig. 68. The external dominant foliation is deflected around the intrusion, but at the same time is axial planar to the fold and can be correlated with the internal magmatic to solid state fabric and with the compositional banding in the granitoid. (b) The magmatic to solid state fabric in the quartz-dioritic body is parallel to different compositional heterogeneities. A leucogranite dyke cross-cuts it with sharp contacts but includes some of the deformational fabric in the more basic intrusion.

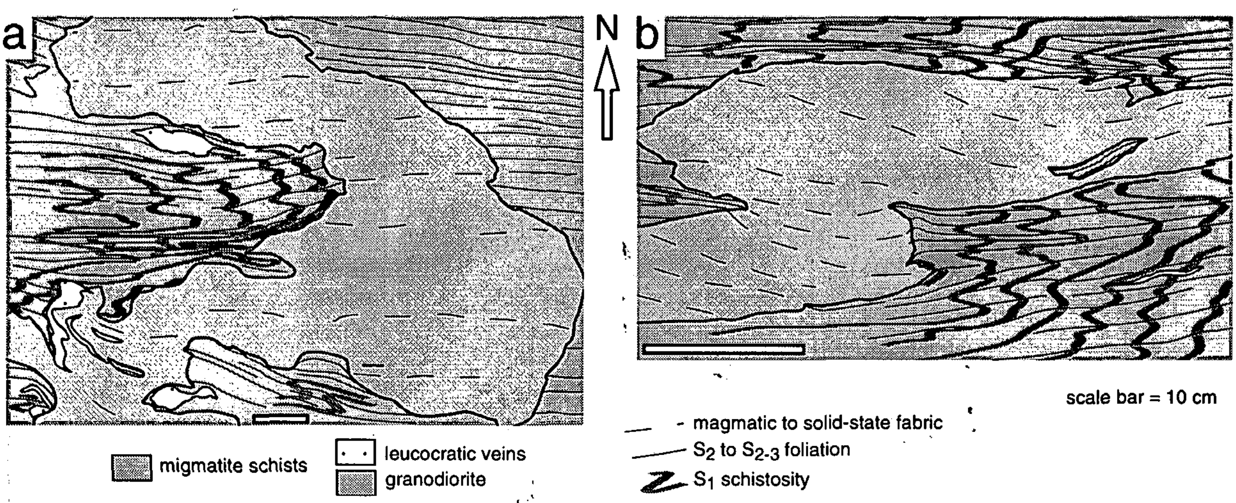

Fig. 70. Field sketches. (a) A small granodiorite body with fold-like shape. The internal fabric is parallel to the external transposition foliation and axial planar of the folds. (b) Granite vein slightly oblique to $S_2 \pm S_{2-3}$ foliation. In this case, the internal magmatic fabric is also slightly oblique to the vein walls and to the crenulation foliation. The vein is containing a small metasedimentary xenolith which carries D_2 deformation features and is aligned parallel to the internal magmatic fabric.

The leucogranites and pegmatites

Both types increase in abundance and size towards the higher grade and higher strain areas. The leucogranites are relatively small (between 5 cm and 5 m in width) and the pegmatites are often larger (between 5 cm and 50 m in width). All these bodies are vein or dyke-like, but many, in addition, have beaded or boudinaged shapes, or occur in networks of foliation-parallel / foliation-oblique veins and dykes, suggesting bridge structures related to dyke emplacement (Fig. 68a). These mainly sub-vertical E-W intrusions are nearly parallel to the axial planes of folds (Fig. 71a) and/or to the D_2 dominant foliation in the country rocks. In the leucogranites, an internal magmatic-state fabric, marked by the preferred orientation of biotite and feldspar, occurs as a continuation of the country rock foliation and, where leucogranites rarely cross-cut the external fabric, they are folded with the magmatic state fabric being axial planar (Fig. 71b), indicating syntectonic emplacement.

There are rarely any magmatic-state fabrics in the pegmatites, because of the massive nature of their crystals and the common occurrence of crystal growth preferred orientation at right angles to vein walls. However, in some of the largest pegmatites, a magmatic banding parallel to the external pervasive foliation can be observed. In the rare cases where dykes have intruded at high angles to the dominant foliation, they have been folded (Fig. 71c & Fig. 68b), but often locally cross-cut the external fabric. The folds of the dykes are coaxial with those in the country rocks but more open, indicating that some deformation had occurred before pegmatite emplacement, and that it continued afterwards.

In areas adjacent to the migmatite outcrops (i.e. Cala Prona zone), some pegmatite dykes are straight, undeformed and cross-cut the transposition foliation in the enclosing metasediments. Assuming that all dykes might have been emplaced close in time, such undeformed ones could represent either the latest intrusions or better syn-$D_{2\text{-}3}$ intrusions in areas of D_2 high strain and very low or scarce $D_{2\text{-}3}$ deformation (see also section 5.3.).

In conclusion, the leucogranites and most of the later pegmatites were emplaced during the same deformation history as the calc-alkaline suite. However, the earlier calc-alkaline units often cross-cut each other with rather vague and diffuse contacts, suggesting a small temperature interval between the respective times of emplacement. On the contrary, the sharp and often fine grained contacts of the later peraluminous bodies where they cut the earlier calc-alkaline units (Fig. 69b and Fig. 71d), suggest that whilst both sequences were emplaced syntectonically, the peraluminous units were well separated in time from the earlier calc-alkaline units.

5.2.2. MIGMATITES AND DEFORMATION

A number of general and specific relationships, illustrating the relative timing of migmatite formation and the regional D_2 deformation, will be shown.

In general terms, it can be seen that as the D_2 strain and transposition increases towards the north, so the more pelitic layers progressively become migmatites. Firstly, the metapelites develop tight folds (Fig. 72a) and a penetrative S_2 foliation, marked by the preferred orientation of biotite, which wraps around early cordierite porphyroblasts. New prismatic sillimanite grows parallel to this fabric. Secondly, S_2-parallel quartz veins, which are abundant on the margins of the pelitic layers, are, on moving northwards into the migmatite zone, progressively replaced by quartzofeldspathic veins (Fig. 70a) or migmatitic leucosomes forming stromatic migmatites. In the northernmost outcrops, the migmatites themselves consist of lensoid or beaded leucosomes surrounded by mafic selvages (Fig. Fig. 72b & c). All this indicates a spatial and, by inference, temporal connection between D_2 strains and in situ migmatization.

On a more detailed scale, a common feature of the calc-alkaline granitoid bodies is their association with melting and assimilation of the country rocks, giving up to "injection migmatites". Often one can see within one outcrop:

a) schists and metagreywackes in the wall-rocks containing D_2 deformational features (folds and cleavages)

b) angular xenoliths of the country rocks containing obvious D_2 structures within the bodies and close to their margins (Fig. Fig. 71e)

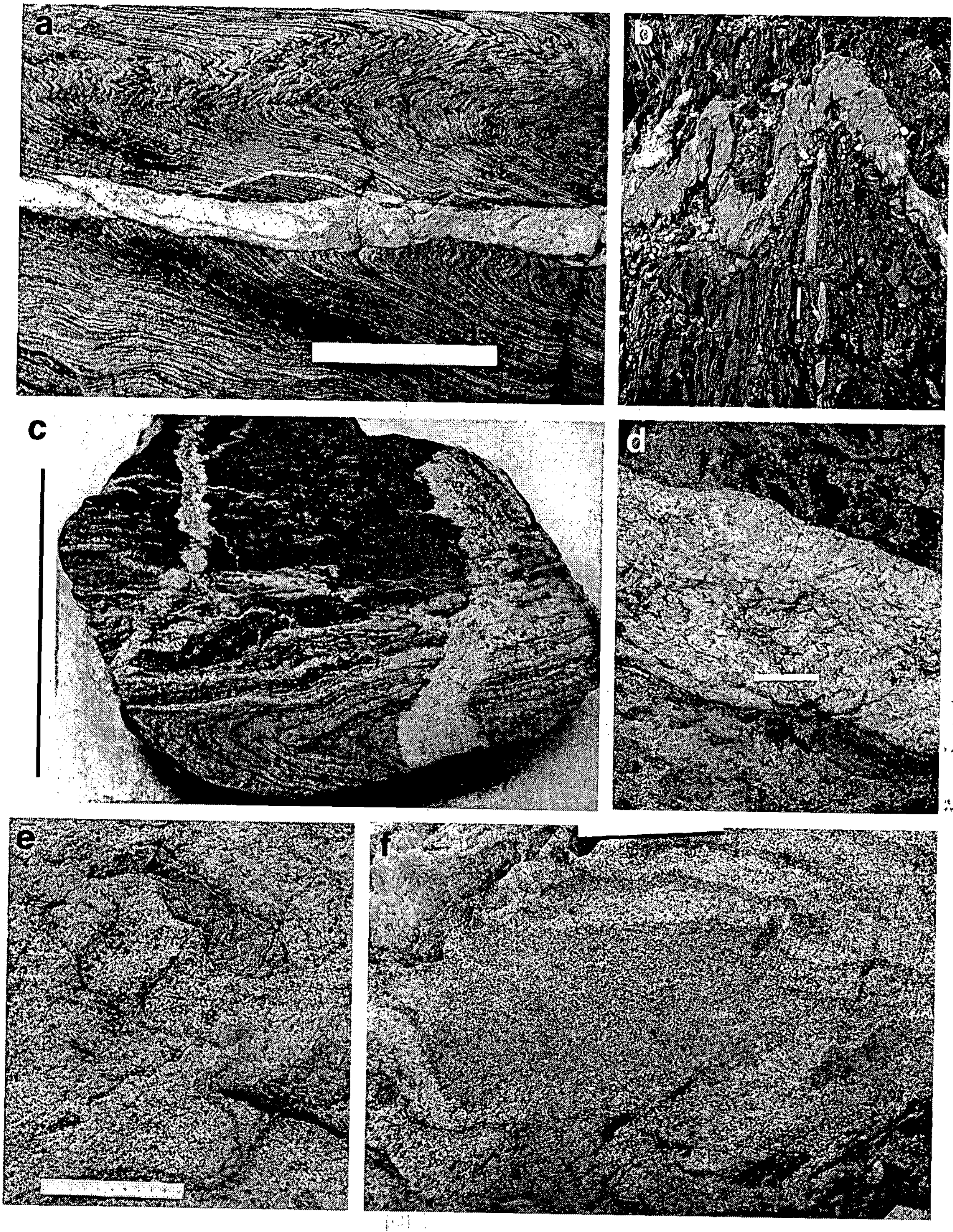

Fig. 71. Field photographs. Scale bar is 10 cm. (a) Leucogranite vein parallel to the axial plane of folds in metagreywackes. (b) Folded leucogranite dyke with axial planar S_2 foliation in the enclosing migmatite schists. The internal magmatic state fabric may be correlated with the S_2 foliation. In the center of the photograph, a boudined leucocratic vein intrudes parallel to S_2 foliation. (c) Pegmatite veins coaxially folded with the enclosing metasediments but with a more open shape. (d) Pegmatite dyke sharply intruded into an enclave-rich granitoid. (e) Garnet-rich granodiorite-tonalite containing a small angular metasedimentary xenolith which displays F_2 folds. (f) Within the same intrusion, the country rock xenoliths have become more rounded and the original deformational texture has almost disappeared and/or has been substituted by a new S_2-parallel fabric.

c) further within the intrusions, the country rock xenoliths have lost their angular nature and have become more rounded

d) within these more rounded xenoliths, the D_2 structures are very vague and vestigial, and the original deformational texture has almost disappeared (Fig. 71f)

e) there are other such xenoliths where the internal D_2 structures have completely disappeared.

This suggests that the xenoliths have come close to complete melting before crystallizing again, i.e. they have been "mobilised" (Pitcher & Berger 1972). In addition, the igneous bodies often carry a D_2 fabric which may deform the mobilised xenoliths. This suggests that intrusion, deformation and near-melting are all contemporaneous.

5.2.3. DISCUSSION ON SYNTECTONIC MAGMATISM AND MIGMATIZATION

The coexistence of the migmatite complex with a contemporaneous zone of high-strain is good evidence of a connection between deformational and magmatic processes. The studied relationships between structures (folds, crenulation cleavage and transposition foliation) in the metasediments and the internal deformational fabrics in the granitoids and migmatites support the synchronicity of deformational processes, magmatism and migmatization. The magmatic fabrics and banded compositional heterogeneities present in some intrusive bodies and dykes can be easily correlated with the pervasive foliation in the country rocks. Moreover, dyke walls are either in close parallelism with the axial planes of the folds (or with its cogenetic foliation) or they are coaxially folded with a more open shape than the nearby metasediments.

In addition, the relative timing of emplacement is given by the analysis of cross-cutting relationships between different granitoids. The more acid types always cross-cut the rocks of the intermediate-basic sequence. This fact, together with the observation of different degrees of deformation (with the earliest granitoids recording larger strains than the latest ones), verifies that magmatism in this area took place as synkinematic consecutive intrusions from the more basic magmas to the peraluminous acid dykes.

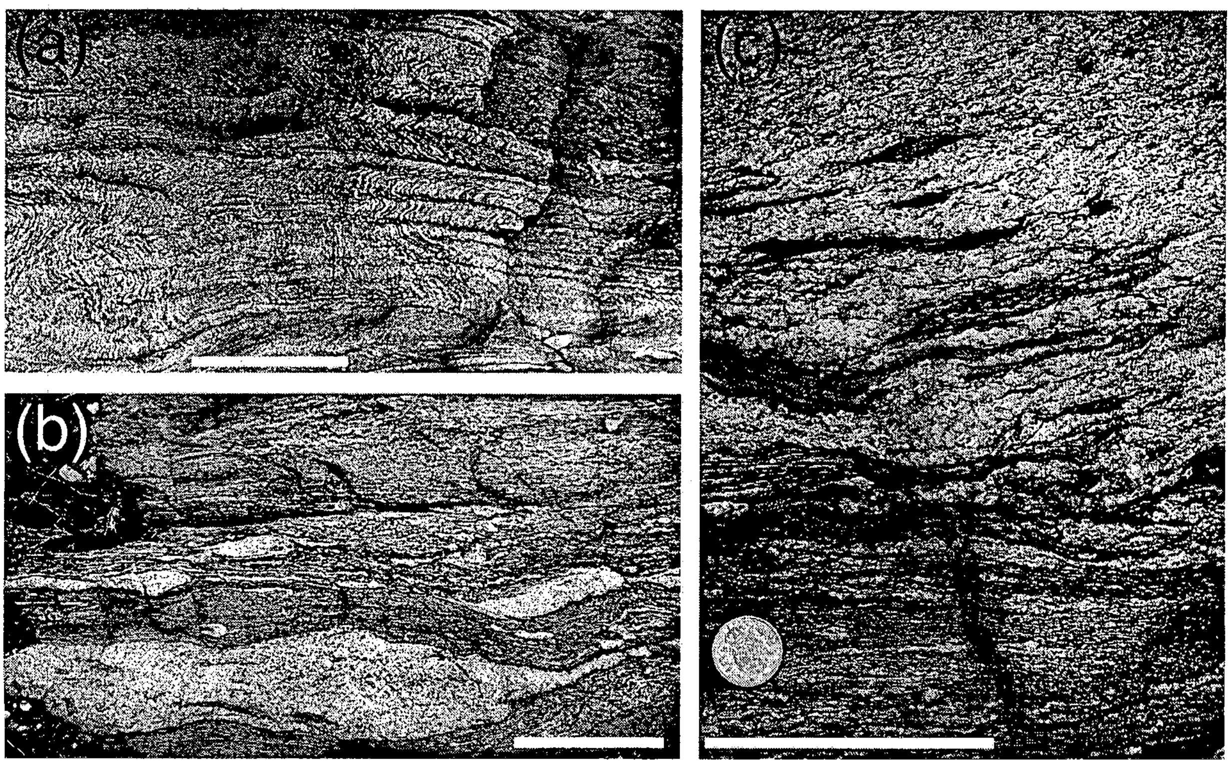

Fig. 72. Field photographs. Scale bar is 10 cm. (a) Folds and related crenulation cleavage affecting the metagreywackes. (b) Metapelites are transposed and beaded leucosome veins develop in close parallelism with S_2. (c) Transition from a stromatic migmatite (lower part of the photograph) to a schlieren migmatite and more homogeneous granite (upper part). The layered structure corresponds to the S_2 foliation and is well defined by biotite-rich melanosomes.

The rocks of the calc-alkaline sequence probably intruded as subvertical lensoid bodies, oblique to S_2 and along D_2-related tension fractures, Riedel shears and/or following the S_1 fabric. These intrusions were folded by the progressive D_2 to D_{2-3} deformation. During the last stages of the D_2 deformation (i.e. during D_{2-3} stage), leucogranite and pegmatite dykes were injected along foliation-oblique tension fractures or into bridges between P-shears (Tikoff & Teyssier 1992), but also by using the already existing S_2 surfaces as planes of major weakness. The present day close parallelism of most of the lensoid bodies and dykes to the dominant foliation is either a result of strong deformation of the first intrusions or a result of the latest injections along S_2 weakness planes.

As regards the origin of the migmatites in this area, they are probably formed by two different, but ultimately related, processes. Firstly, by in situ partial melting of the most pelitic metasediments in the zones of highest strain. Secondly, melting is induced by the small scale granitoid bodies, also during deformation. However, given that the calc-alkaline granite bodies are restricted to the high grade metamorphic and migmatite zone, and that they were intruded during the D_2 deformation, which was also the time of formation of the migmatites, then, it seems possible that the heat source for the in situ migmatites was the presence of nearby granitoid bodies at depth.

5.3. PEGMATITE DYKE SWARM AND DEFORMATION

The pegmatite dyke swarm, located in medium and high grade metamorphic zones, will be described in this chapter from a structural point of view. A close look to the structures displayed by pegmatites and their relationships with deformations recorded by the adjacent metasediments has provided much information on the relative timing of emplacement of these dykes and the deformation events, and on the time relationships of the successive deformations themselves.

A first delimitation places the time of emplacement of these dykes between D_1 and D_3 deformation events. Indeed they exhibit clear cross-cutting relationships with respect to the bedding and S_1 foliation and are deformed at low temperature solid state by D_3 late deformations (Fig. 73). Dykes may develop into F_3 folds with a penetrative axial planar foliation or be displaced by shear zones. Within late shear zones, some dykes show a characteristic mylonitic foliation. Secondly, as described in the previous section, pegmatites cross-cut the granitoids of the migmatite complexes. These granitoids already carry xenoliths with F_2 folds. From these observations, it is deduced that the pegmatite dyke swarm was emplaced mainly in synchronicity with the D_{2-3} deformational stage.

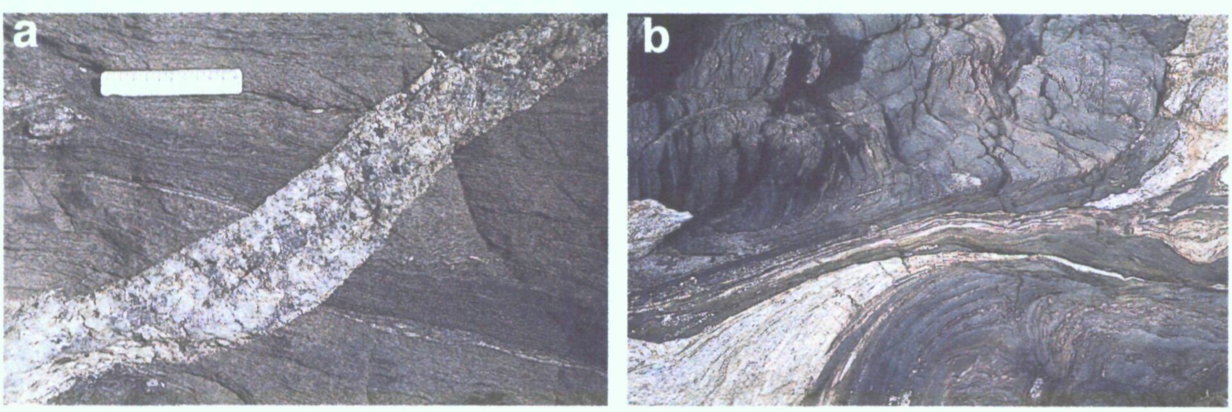

Fig. 73. Pegmatite vein cross-cutting the bedding-parallel S_1 foliation (a, Canal Guillosa) and pegmatite dyke deflected and deformed by a late shear zone (b, Es Conill).

In map view (Fig. 11 and Structural Map), pegmatite dykes are heterogeneously distributed along and across a rough band trending approximately E-W. The location of the largest and most abundant pegmatite dykes coincides approximately with the zones of high D_2 to D_{2-3} strain. In these zones, dykes are abundant (occupying up to 15-20% of the total horizontal area), and form huge bodies up to a few hundred meters long and 100 m wide (Fig. 74). In domains of low D_2 and D_{2-3} strain they are scarcer and smaller except in the zones adjacent to higher strain domains. Then, the space distribution of pegmatites is not only related to the metamorphic zonation but also to the structural zonation. The D_{2-3} folding event, and the associated strain distribution, controlled the emplacement of the syntectonic pegmatite dyke swarm.

Fig. 74. Aerial photograph of the Culip-Cullaró area, showing pegmatite bodies (white). Width of view 500 m.

Pegmatites occur mainly as sub-vertical planar dykes or more irregularly shaped elongate bodies. Some sub-horizontal or gently dipping pegmatite dykes are also present, and these are often connected to vertical veins which seem to have acted as feeder dykes. The stereoplot in Fig. 75 show orientations of pegmatite dykes. Only undeformed dykes plus those affected by D_{2-3} syn- to post-magmatic deformation have been plotted. They are predominantly sub-vertical and range in orientation from N-S to E-W, a majority of them being close to E-W.

The shape, orientation, size and strain recorded by these dykes considerably varies from one structural setting to another, so that the description of these features will be made for three different structural situations. Although much more complicated scenarios may exist, their discussion would not change the basic principles here illustrated.

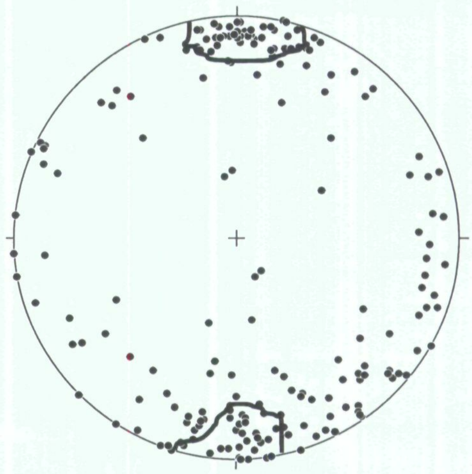

Fig. 75. Equal area lower hemisphere projections of poles to pegmatite dyke walls. N=225. 4% contour is shown. Pegmatites deformed by D_3 late folds and shear zones have not been plotted.

5.3.1. PEGMATITES IN DOMAINS OF PROGRESSIVE D_2 TO D_{2-3} DEFORMATION

The cases with pegmatites emplaced in structural settings where deformation took place in a progressive way from D_2 to D_{2-3} stage are the most widespread. This is the case, for instance, of the Culip-Cap de Creus area (Carreras & Druguet 1994a, Druguet et al. 1997), exposed in section 4.4.1, and the Punta dels Farallons area just described.

In the lower strain domains, where S_1 is the dominant foliation, some pegmatites are emplaced sub-parallel with S_1 in domains of local fold intensification (Fig. 76b, c and Fig. 77a, b). Such pegmatites are coaxially folded with the enclosing metasediments but with a more open form, with abundant examples of pegmatite fold patterns analogous to the example described by Ramsay (1967, Fig. 7-2, p. 344). No penetrative solid state tectonic fabric is present in the folded pegmatites, indicating that folding may have taken place when the pegmatites were still partly in a melt or fluid state. Other dykes are emplaced obliquely to the S_1

foliation and at a low angles to the crenulation cleavage, displaying beaded shapes that resemble pinch-and swell structures (Fig. 76d and Fig. 78). Cuspate-lobate structures (Ramsay 1982) around folded and stretched pegmatites indicate a more competent behaviour of the magmatic crystal mush than the enclosing metasediments.

Towards higher strain domains, where folds become tighter in the metasediments until the development of the transposition foliation, pegmatites are more abundant. Dykes and more irregular bodies generally exhibit an elongate shape, with their long axis in close parallelism with the trend of the transposition foliation, which sometimes envelopes the lenticular bodies. However, S_2-oblique dykes are also present, in which case they are systematically folded (Fig. 77c). Boudinage (or pinch and swell), and folding of the pegmatites show similar relationships as in lower strain domains, enabling us to conclude that the dykes were also synkinematically emplaced here. The major form and orientation of pegmatite were probably established during the intrusive phase, and were altered during subsequent deformation. Pegmatites at a high angle to the crenulation foliation are folded and those at a low angle are stretched.

Fold and boudin asymmetries depend on the angular relationships between the $S_{s/1}$ schistosity, the crenulation foliation and the pegmatite vein. Besides, in some outcrops, the location of boudin necks can be seen to coincide with psammitic layers (Victor 1996, Druguet et al 1997). Boudinage is either developed as pinch-and swell type or as separated boudins (Fig. 79). In the last case, the continuity of psammitic layers without scars between boudins indicates that some pegmatites were injected forming strings of lens-shaped pods. Stretch values up to S=2 (measured on horizontal outcrop faces) have been obtained from stretched pegmatites in the higher strain zones. Boudinaged pegmatites are axial planar to folds in the enclosing schists (Fig. 77d). Moreover, some complex fold structures of S_1 only occur adjacent to boudins in pegmatites. These structures, analysed in very detail by Victor (1996), are interpreted as being due to complex progressive deformation close to the pegmatites during and after the time of intrusion.

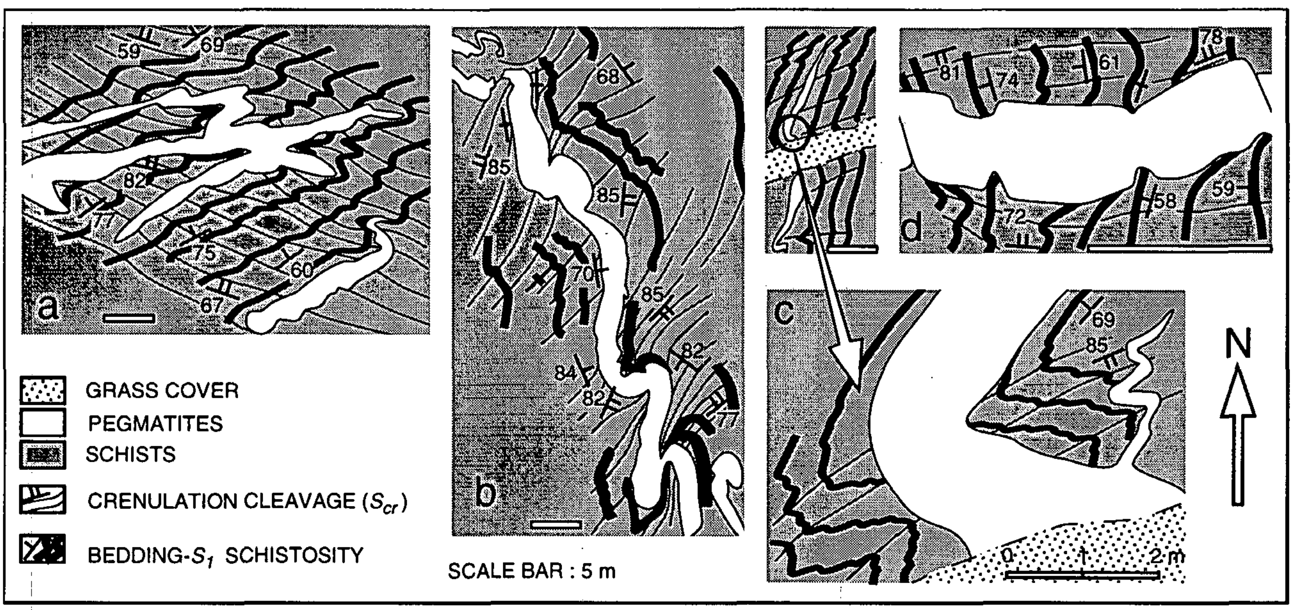

Fig. 76. Different shapes of pegmatite dykes in the Culip area. (a). Complex pegmatite body with differently oriented apophyses. (b). Cuspate structures in a bedding parallel pegmatite. The dyke forms a relatively high angle with the crenulation cleavage (Scr). (c). Similar setting to (b) with detail of S_1-dyke relationship. (d). Pinch and swell pegmatitic dyke crosscutting bedding-S_1 at a high angle. The trend of the dyke is closely parallel to Scr. After Carreras & Druguet (1994b).

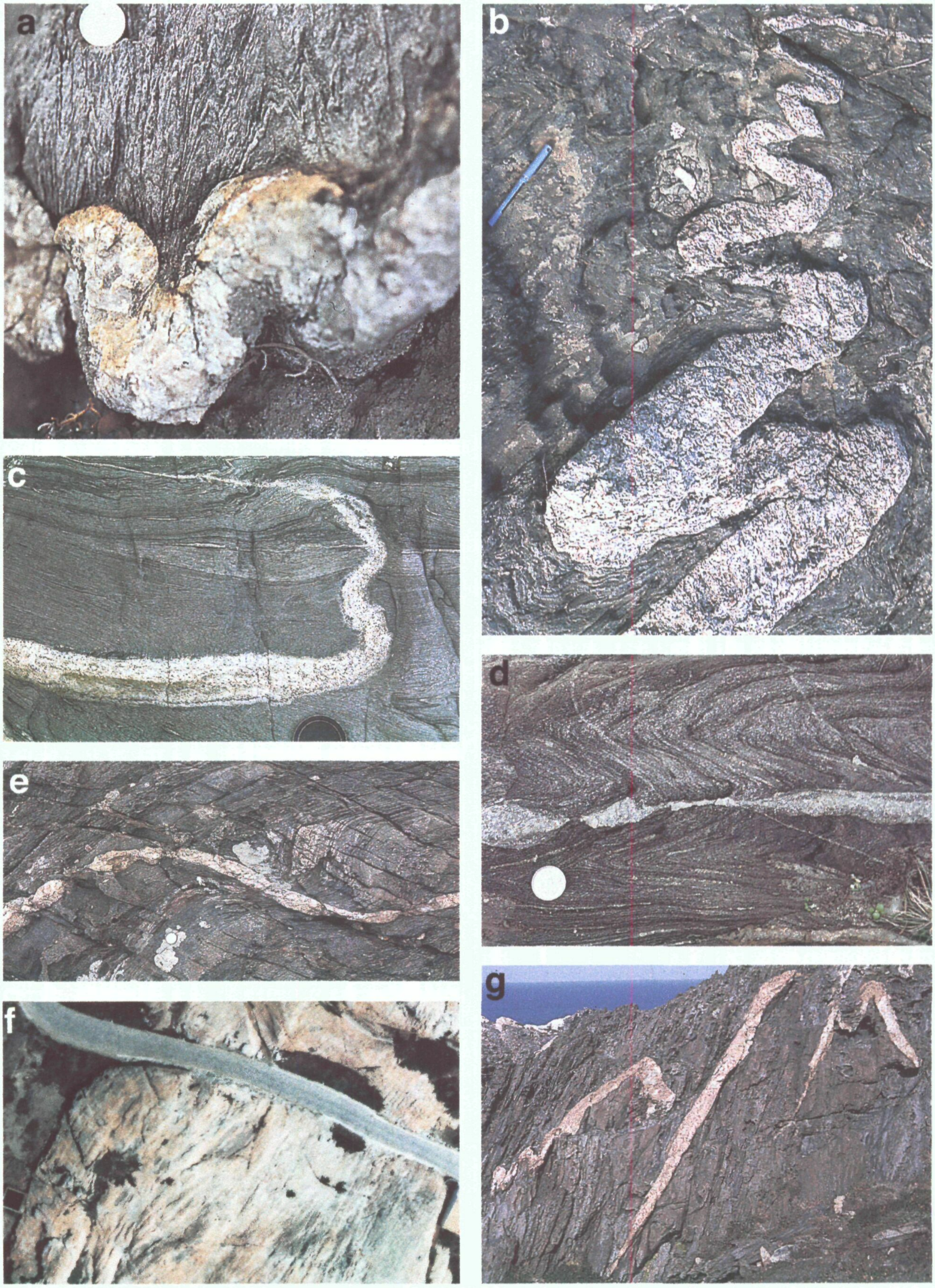

Fig. 77. Field photographs on relations between pegmatite dykes and regional deformation. (a): Syntectonically folded pegmatite vein. Folds in schists and pegmatite are coaxial but differ in tightness (Puig de Culip). (b): Folded pegmatite dyke. Notice the effects of the variable dyke thickness in controlling the folds wavelength (west Puig d'en Melus). (c): Pegmatite vein emplaced in a domain of D_2 to $D_{2\text{-}3}$ progressive deformation (south Volt Andrau). The S1 foliation is isoclinally folded, whereas the vein records shorter amount of deformation. (d): Boudinaged pegmatite vein, parallel to the axial plane of the folds in the schists (south Volt Andrau). (e): Pegmatite vein emplaced along the sheared limb of a fold (lighthouse). (f): Aerial photograph of a pegmatite body from Tudela, showing internal lines which correspond to a compositional banding. These bands are parallel to the pervasive tranposition foliation in the enclosing metasediments. Width of view 140 m. (g): Folded pegmatite dykes in a vertical section (south Cala Cullaró). Width of view 30 m.

Enclaves and different compositional inhomogeneities in the larger bodies or dykes are in close parallelism with the transposition foliation (Fig. 77f), and this is another criterion for the syntectonism of pegmatites (see Vernon et al. 1989).

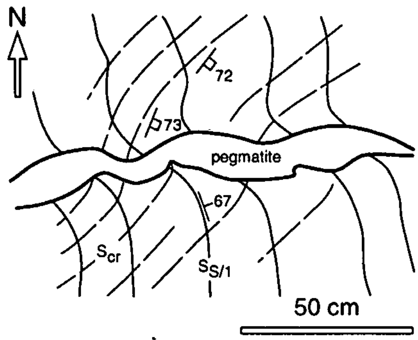

Fig. 78. Field sketch of a pegmatite vein emplaced at a high angle to the S_1 foliation and at a low angle to the crenulation cleavage (Scr). Note the pinch-and swell structure. South of Cala Fredosa (map view).

The intersection lineation of the predominant sub-vertical pegmatite dykes with S_1 and S_2 and the intersection lineation of both foliations are all subparallel and sub-vertical. Most of the dykes also develop a subvertical to steeply west plunging stretching lineation, which is also parallel to L_2 and $L_{2\text{-}3}$ lineations. Moreover, both fold axes and boudin necks (in folded and stretched dykes respectively) have equally steep plunges and, therefore, are subparallel or at low angle to the stretching lineation.

Boudinage parallel to the prevalent steep stretching lineation is much less frequent. The few sub-horizontal to gently dipping dykes can also display fold structures, observed in vertical sections (Fig. 77g). Once more, folds are more open in the pegmatites than in bedding-S_1 foliation but, in these cases, they differ in axis orientation. This has been illustrated in Fig. 80 where one can see the different position of fold axes on a sub-vertical quartzite layer and on a sub-horizontal pegmatite vein.

Some pegmatites have contact zones that are enriched in tourmaline (Fig. 81a). Where pegmatite cuts through alternating micaschists and sandstones, tourmaline rich rims (TRR) are only developed in the micaschist, due to transformation of mica into tourmaline (Victor 1996, Druguet et al. 1997). The angular relationships between S_1 foliation and pegmatite walls at the time of the intrusions are sealed at the TRR. In zones with higher strain, the ghost foliation in TRR is commonly oblique to S_1 in the wall rock, indicating relative rotation of dykes (with their TRR) and S_1 in the wall rock during $D_{2\text{-}3}$ and just after pegmatite was completely crystallized. Inferences from these particular structures for the strain and kinematics of the $D_{2\text{-}3}$ stage will be discussed in the next chapter.

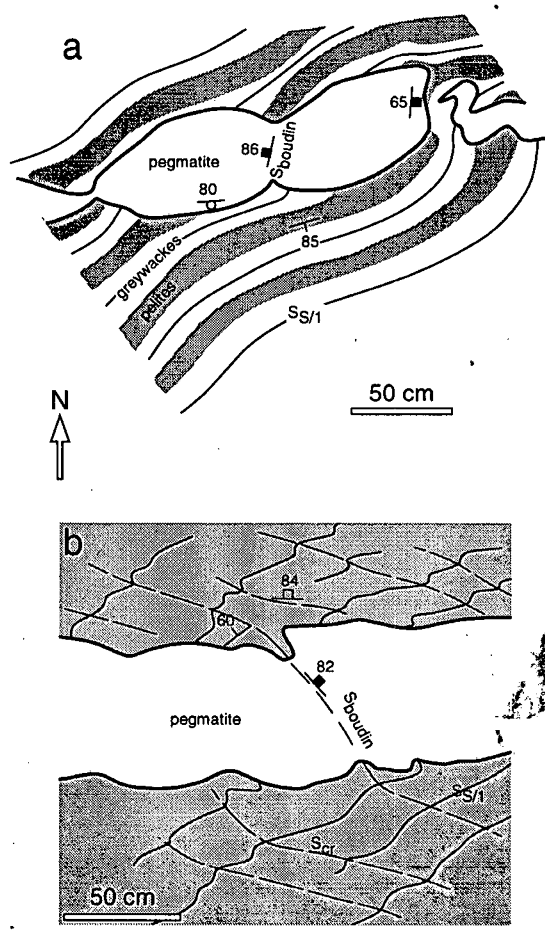

Fig. 79. Field sketches of boudinage structures in pegmatites from medium strain domains (map view). In (a), the continuity of greywackic layers without scars between boudins indicates that the pegmatite was injected forming strings of lens-shaped pods (lighthouse zone). In (b), asymmetric boudinage is developed as a pinch-and swell type. The neck surface is in continuity with the crenulation cleavage (Scr) in the enclosing metasediments (south Cullaró).

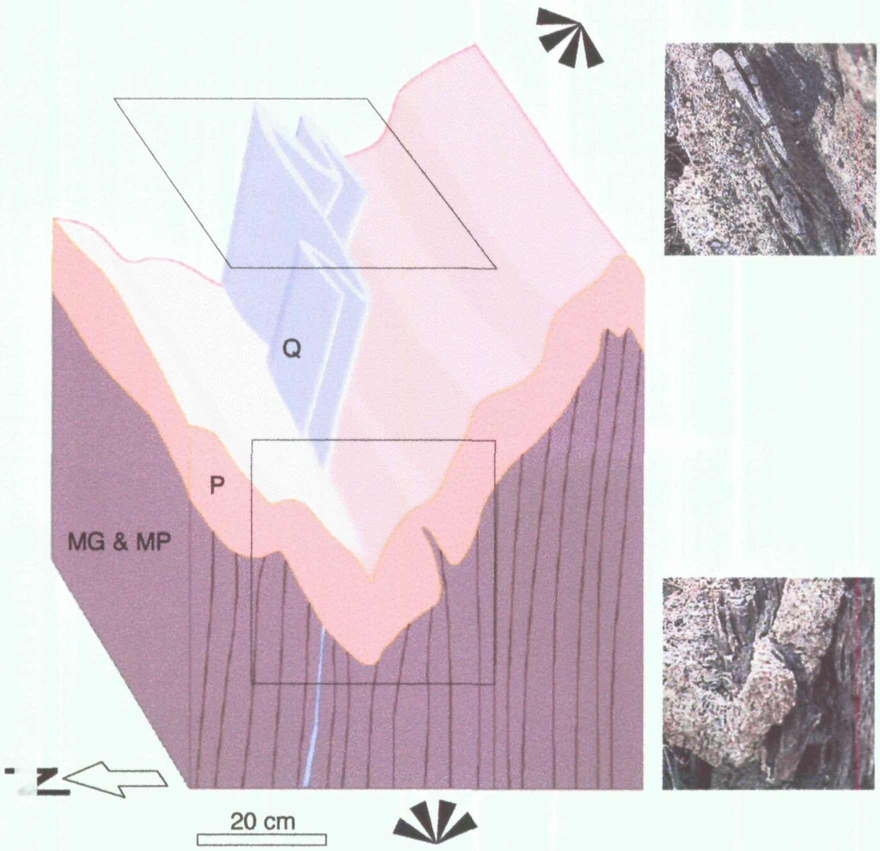

Fig. 80. Three-dimensional sketch of the relationships between folding of a sub-horizontal pegmatite dyke and of a sub-vertical quartzite layer (lighthouse area). Folds are more open in the pegmatites than in the quartzite and differ in axis orientation. Photographs of the structure in horizontal and vertical views are also shown. MG & MP=metagreywackes and metapelites, Q=quartzite, P=pegmatite

5.3.2. PEGMATITES IN DOMAINS OF LOW D_{2-3} DEFORMATION

The lesser deformed pegmatite dykes have been observed in domains of medium to high D_2 strain and very low or scarce D_{2-3} deformation. NE-SW to NW-SE trending dykes are sub-vertical, straight and cross-cut the D_2 folds and the transposition foliation which trends NE-SW in these domains.(Fig. 81b, c). Some dykes seem emplaced following the already existing S_2 surfaces as planes of major weakness. Others would have been injected along tension fractures oblique to the S_2 foliation. In both cases, the dilatation direction was normal or at least highly oblique to the dyke walls, since there is no offset of bedding and other markers, and since tourmaline crystals inside pegmatites are commonly normal to their walls (Fig. 81d).

5.3.3. PEGMATITES IN DOMAINS OF OVERPRINTING OF D_2 BY D_{2-3}

The progressive D_2 to D_{2-3} regional deformation was accompanied by inhomogeneous strain and thus leaded to the isolation of few domains with D_2 structures overprinted by D_{2-3} (section 4.4.2). Pegmatite dykes emplaced in these settings clearly cross-cut D_2 folds while displaying syn-kinematic features with respect to D_{2-3} deformation (Fig. 81e). The most illustrative examples are located in the northern and southern exposures around Cala Galladera (Structural Map and Fig. 50). Several large E-W pegmatite sheets are steeply dipping to the north, cross-cutting D_2 isoclinal folds at a high angle. Some apophyses or branches depart from the E-W pegmatites in a direction parallel to the S_2 foliation, possibly by using these surfaces as planes of weakness. Both oppositely oriented types of dykes show an internal magmatic compositional banding parallel to their walls. The E-W ones display pinch- and swell structures, whereas the closer to N-S are straight or slightly folded. Hectometric E-W folds and related crenulation cleavage, dated as corresponding to the D_{2-3} event, seem genetically associated to the E-W pegmatite sheets. This pattern, also shown in more detailed scales in Fig. 82, is analogous to that observed in domains of progressive D_2 to D_{2-3} deformation (section 5.3.1), with complex fold structures only in areas adjacent to pegmatites. Both patterns differ, however, in the nature of the dominant foliation at the onset of the D_{2-3} stage, which was the S_2 foliation in this place and the bedding/S_1 in the former case. Xenoliths of country rocks within the largest pegmatites have an E-W preferred orientation and usually include D_2 deformational features (foliations and isoclinal folds). These are deflected towards the contacts of the enclave and are tighter in the tails of the elongate xenoliths (Fig. 82a). These structures can be correlated with $D_{2\text{-}3}$ folds outside of the pegmatites and are therefore interpreted as developing during pegmatite intrusion.

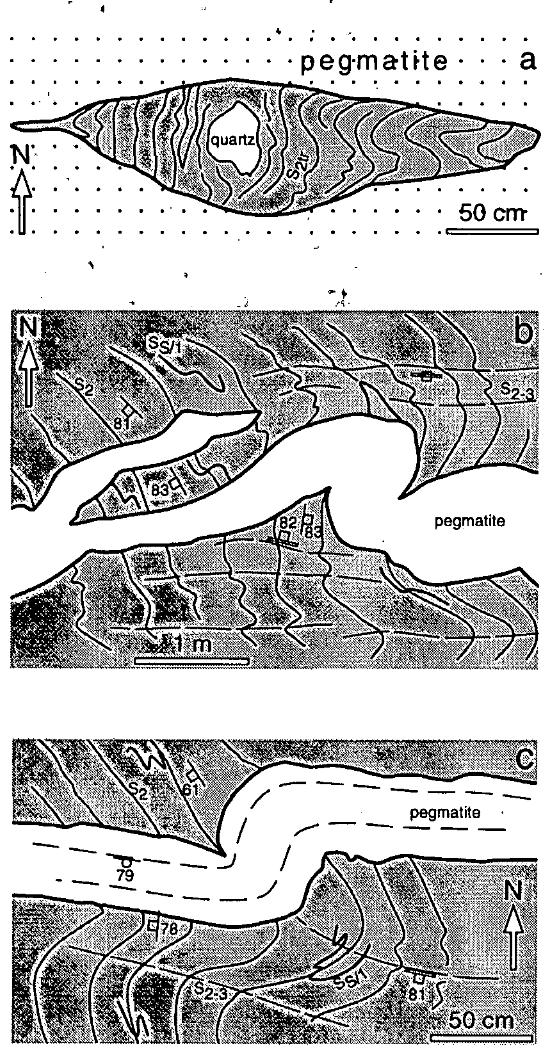

Fig. 82. Field sketches of structures related to pegmatite dykes emplaced in domains of overprinting of D_2 by $D_{2\text{-}3}$ (Canal Guillosa-Cala Galladera, map view). (a): a metasedimentary xenolith within a pegmatite dyke displays D_2 (transposition foliation, S_{2tr}) and $D_{2\text{-}3}$ structures (see also text). (b & c): dykes cross-cutting the S_2 foliation at a high angle and displaying $D_{2\text{-}3}$ deformational features (cuspate-lobate folding and boudinage). Dashed lines in (c) indicate compositional bands within the dyke.

5.3.4. THE EMPLACEMENT OF THE PEGMATITE DYKES

Although there is a certain degree of preferred orientation of pegmatite dykes parallel to the trend of the higher strain domains, no a single geometry seems to govern the opening of the space occupied by the pegmatites. It appears that some of the pegmatite bodies have side-walls disposed parallel to the dominant foliation in plane view, which can be either the bedding-S_1 foliation or the D_2 transposition foliation, indicating that pre-existing planes of weakness were major controlling elements. According to Brisbin (1986), in ductile domains, ductility anisotropies, rather than tensile-strength anisotropies, may control the intrusion of pegmatites. Consequently, pegmatite intrusion may follow a foliation or may be confined to a more ductile layer. High-strain zone anisotropy was probably an important factor controlling dyke orientations during the latest stages of emplacement (see Hutton 1992) and the steeply plunging stretching direction (i.e. transport direction) may have facilitated melt ascent.

In some instances, pegmatite dykes cut across the dominant foliation, possibly following tension fractures. In such a situation, dykes are also subjected to folding and/or boudinage by progressive deformation.

The abundance of melts parallel to the axial planes of the $F_{2\text{-}3}$ folds is comparable to many smaller scale structures with axial-planar leucosomes, leucogranites or pegmatites described in similar structural settings (e.g. Edelman 1973; Ramsay & Huber 1987, Fig. 20.12, p. 416; McLellan 1988; Hudleston 1989; Passchier et al. 1990; Hand & Dirks 1992). According to Hand & Dirks (1992), vertical crenulations represent an ideal orientation for buoyancy-driven melt drainage. At larger scales, similar relationships between deformation and melting have also been described (see Pitcher 1979, Hutton & Reavy 1992).

In the next chapter, the use of the structures generated in differently oriented dykes will furnish more insights on the vorticity of deformation and the bulk tectonic regime of the area.

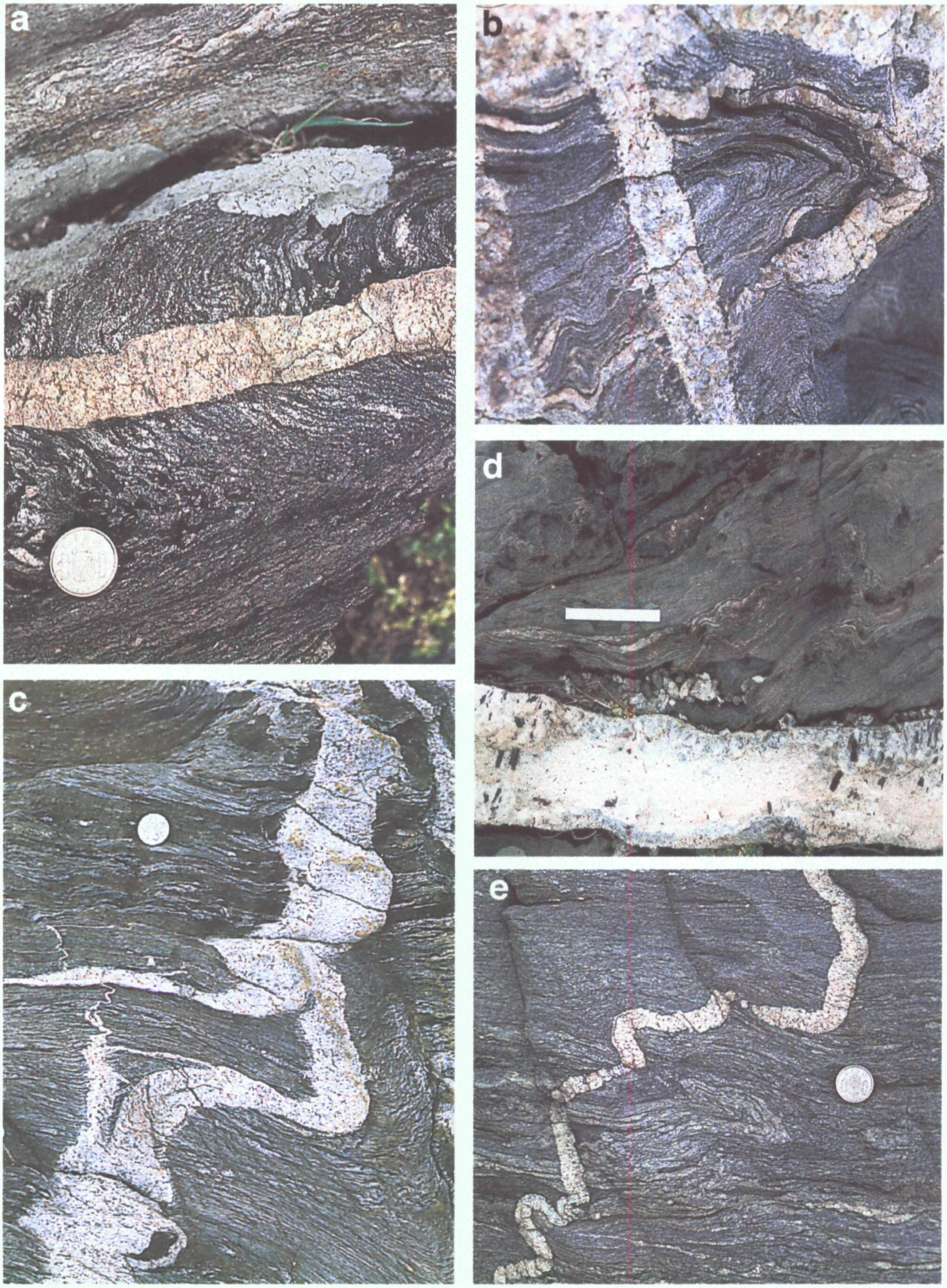

Fig. 81. Field photographs of relations between pegmatite dykes and deformation. (a): Pegmatite vein with tourmaline rich rims (lighthouse zone). See explanation in text. (b): Straight apophysis of a large pegmatite body, cutting a F_2 fold (between Cala Portaló and Mas Rabassers de Baix). Width of view 30 cm. (c): Pegmatite dyke and veins emplaced at a high angle to a S_2 transposition foliation (NE Mas de la Birba). They display open folds due to D_{2-3} deformation. (d): Straight dyke containing tourmaline crystals with their long axes normal to the dyke walls (west Puig de Cala Sardina). Scale bar = 10 cm. (e): Pegmatite vein cross-cutting D_2 isoclinal folds. The schists show refolded folds due to D_{2-3} overprinting, whereas the vein is syntectonically folded in regard to the D_{2-3} stage (south of Volt Andrau).